

for this interface architecture. Another underestimated degradation mechanism we propose is the reaction between the I_2 from perovskite and the HTMs with HOMO levels of around -5.0 eV near the oxidation potential of I^-/I_3^- . After a 2-min exposure to I_2 vapor, both P3HT and spiro-MeOTAD films exhibited notable color changes, which we mainly attributed to their polaron absorption after reaction with I_2 . In strong contrast, PDCBT maintained its purple color unchanged (Fig. 4I), which demonstrates its robustness under I_2 vapor treatment due to a lower HOMO level approaching -5.3 eV. All of these findings highlight the importance of the deep HOMO level of HTMs (Fig. 4J) in efficient and stable perovskite solar cells and lead us to properly design heterojunction interfaces for perovskite solar cells with enhanced efficiency and longevity.

REFERENCES AND NOTES

- National Center for Photovoltaics (NCPV) at the National Renewable Energy Laboratory (NREL), "Best research-cell efficiencies"; www.nrel.gov/pv/assets/images/efficiency-chart.png (2017).
- H. J. Snaith *et al.*, *J. Phys. Chem. Lett.* **5**, 1511–1515 (2014).
- T. M. Brenner, D. A. Egger, L. Kronik, G. Hodes, D. Cahen, *Nat. Rev. Mater.* **1**, 15007 (2016).
- B. Hailegnaw, S. Kirmayer, E. Edri, G. Hodes, D. Cahen, *J. Phys. Chem. Lett.* **6**, 1543–1547 (2015).
- C. Eames *et al.*, *Nat. Commun.* **6**, 7497 (2015).
- F. Bella *et al.*, *Science* **354**, 203–206 (2016).
- X. Li *et al.*, *Science* **353**, 58–62 (2016).
- M. Saliba *et al.*, *Science* **354**, 206–209 (2016).
- E. T. Hoke *et al.*, *Chem. Sci.* **6**, 613–617 (2015).
- M. Saliba *et al.*, *Nat. Energy* **1**, 15017 (2016).
- M. A. Green, A. Ho-Baillie, H. J. Snaith, *Nat. Photonics* **8**, 506–514 (2014).
- C. C. Chueh, C. Z. Li, A. K. Y. Jen, *Energy Environ. Sci.* **8**, 1160–1189 (2015).
- P. Ganesan *et al.*, *Energy Environ. Sci.* **8**, 1986–1991 (2015).
- G. W. Kim *et al.*, *Energy Environ. Sci.* **9**, 2326–2333 (2016).
- Y. Liu *et al.*, *Adv. Mater.* **28**, 440–446 (2016).
- P. Schulz *et al.*, *ACS Appl. Mater. Interfaces* **8**, 31491–31499 (2016).
- P. Liu *et al.*, *Appl. Phys. Lett.* **106**, 193903 (2015).
- J. Xu *et al.*, *Adv. Mater.* **28**, 2807–2815 (2016).
- Y. Hou *et al.*, *Adv. Energy Mater.* **5**, 1500543 (2015).
- See supplementary materials.
- Y. Hou *et al.*, *Adv. Mater. Interfaces* **4**, 1700007 (2017).
- Y. Hou *et al.*, *Adv. Mater.* **28**, 5112–5120 (2016).
- M. Zhang, X. Guo, W. Ma, H. Ade, J. Hou, *Adv. Mater.* **26**, 5880–5885 (2014).
- X. Lan, S. Masala, E. H. Sargent, *Nat. Mater.* **13**, 233–240 (2014).
- J. Gao *et al.*, *Nano Lett.* **11**, 3263–3266 (2011).
- R. C. Shallock *et al.*, *J. Phys. Chem. Lett.* **6**, 1303–1309 (2015).
- K. Zilberberg *et al.*, *Adv. Funct. Mater.* **21**, 4776–4783 (2011).
- J. Meyer *et al.*, *Adv. Mater.* **24**, 5408–5427 (2012).
- K. Domanski *et al.*, *ACS Nano* **10**, 6306–6314 (2016).
- W. Li, W. S. C. Roelofs, M. Turbiez, M. M. Wienk, R. A. J. Janssen, *Adv. Mater.* **26**, 3304–3309 (2014).
- C. Huang *et al.*, *J. Am. Chem. Soc.* **138**, 2528–2531 (2016).
- M. Stollerfoht *et al.*, *Energy Environ. Sci.* **10**, 1530–1539 (2017).
- K. Rakstys *et al.*, *J. Mater. Chem. A* **5**, 7811–7815 (2017).

ACKNOWLEDGMENTS

We acknowledge funding from the SAOT at FAU Erlangen-Nürnberg, which is funded by the German Research Foundation [Deutsche Forschungsgemeinschaft (DFG)] within the framework of its "Excellence Initiative." The work was further supported by the Cluster of Excellence "Engineering of Advanced Materials." We acknowledge financial support from the DFG research training group

GRK 1896 at FAU and from the Bavarian Ministry of Economic Affairs and Media, Energy and Technology, for the joint projects in the framework of the Helmholtz Institute Erlangen-Nürnberg for Renewable Energy (IEK-11) of Forschungszentrum Jülich. We thank O. Lytken, C. O. Ramirez Quiroz, X. Tang, S. Chen, G. J. Matt, and A. Osvet for conducting XPS, UPS, UV-Vis absorption, AFM, electroluminescence, and PXRD characterizations and valuable discussions. Additionally, C.J.B. gratefully acknowledges financial support through the "Aufbruch Bayern" initiative of the state of Bavaria, the Bavarian Initiative "Solar Technologies go Hybrid" (SolTech), and the "Solar Factory of the Future" with the Energy Campus Nürnberg (EnCN). N.L. acknowledges financial support from

the Emerging Talents Initiative at FAU and DFG grant BR 4031/13-1. All data are presented in the main text and supplementary materials.

SUPPLEMENTARY MATERIALS

www.sciencemag.org/content/358/6367/1192/suppl/DC1
Materials and Methods
Figs. S1 to S13
Tables S1 to S4

3 August 2017; accepted 27 October 2017
Published online 9 November 2017
10.1126/science.aao5561

PALEONTOLOGY

Egg accumulation with 3D embryos provides insight into the life history of a pterosaur

Xiaolin Wang,^{1,2*} Alexander W. A. Kellner,^{3*} Shunxing Jiang,¹ Xin Cheng,¹ Qiang Wang,¹ Yingxia Ma,⁴ Yahefujiang Paidoula,⁴ Taissa Rodrigues,⁵ He Chen,^{1,2} Juliana M. Sayão,⁶ Ning Li,¹ Jialiang Zhang,^{1,2} Renan A. M. Bantim,⁶ Xi Meng,¹ Xinjun Zhang,^{1,2} Rui Qiu,^{1,2} Zhonghe Zhou^{1,2}

Fossil eggs and embryos that provide unique information about the reproduction and early growth of vertebrates are exceedingly rare, particularly for pterosaurs. Here we report on hundreds of three-dimensional (3D) eggs of the species *Hamipterus tianshanensis* from a Lower Cretaceous site in China, 16 of which contain embryonic remains. Computed tomography scanning, osteohistology, and micropreparation reveal that some bones lack extensive ossification in potentially late-term embryos, suggesting that hatchlings might have been flightless and less precocious than previously assumed. The geological context, including at least four levels with embryos and eggs, indicates that this deposit was formed by a rare combination of events, with storms acting on a nesting ground. This discovery supports colonial nesting behavior and potential nesting site fidelity in the Pterosauria.

Despite recent progress, the general paucity of pterosaur bonebeds confidently composed of a single species hampers our understanding of several biological questions (1, 2), including their ontogenetic development and reproductive strategy. Only a handful of isolated occurrences of eggs and embryos have been reported so far (2–6). Three-dimensionally preserved eggs include one from Argentina (7) and five from the Turpan-Hami Basin, Xinjiang, northwestern China (8, 9). Extensive fieldwork in this area has revealed not

only an extraordinary quantity of eggs, but also the first pterosaur three-dimensional (3D) embryos, providing new information on the embryology and reproductive strategy of these flying reptiles. The specimens can be attributed to *Hamipterus tianshanensis*, the sole species in this bonebed. The most important section is a sandstone block (3.28 m²) that yielded 215 eggs, but up to 300 may be present, because several more appear to be buried under the exposed ones (Figs. 1 and 2 and figs. S1 to S13). The eggs are in an accumulation without a preferential orientation, clearly showing transport (Fig. 2A). Their external surface shows cracking and crazing, and all are deformed to a certain extent, which indicate their pliable nature (Fig. 2, B to F). Although most eggs are complete, small fissures resulting from decomposition and compression during burial must have occurred because all eggs are filled with sandstone, which ultimately accounts for their three-dimensionality.

No nests were found, precluding the establishment of clutch sizes. However, the large number of eggs indicates that they belonged to several clutches and were laid by different females, which is one plausible explanation for their moderate size variation (table S1). Furthermore, egg size discrepancy is common within

¹Key Laboratory of Vertebrate Evolution and Human Origins, Institute of Vertebrate Paleontology and Paleoanthropology (IVPP), Chinese Academy of Sciences, Beijing 100044, China. ²University of Chinese Academy of Sciences, Beijing 100049, China. ³Laboratory of Systematics and Taphonomy of Fossil Vertebrates, Department of Geology and Paleontology, Museu Nacional–Universidade Federal do Rio de Janeiro, Rio de Janeiro, 20940-040, Brazil. ⁴Hami Museum, Hami 839000, China. ⁵Laboratório de Paleontologia, Departamento de Ciências Biológicas, Centro de Ciências Humanas e Naturais, Universidade Federal do Espírito Santo, Vitória, ES, 29075-910, Brazil. ⁶Laboratório de Biodiversidade do Nordeste, Centro Acadêmico de Vitória, Universidade Federal de Pernambuco, Alto do Reservatório Street, s/n. 55608-680, Vitória de Santo Antão, Pernambuco, Brazil.

*Corresponding author. Email: wangxiaolin@ivpp.ac.cn (X.W.); kellner@mn.ufrj.br (A.W.A.K.)

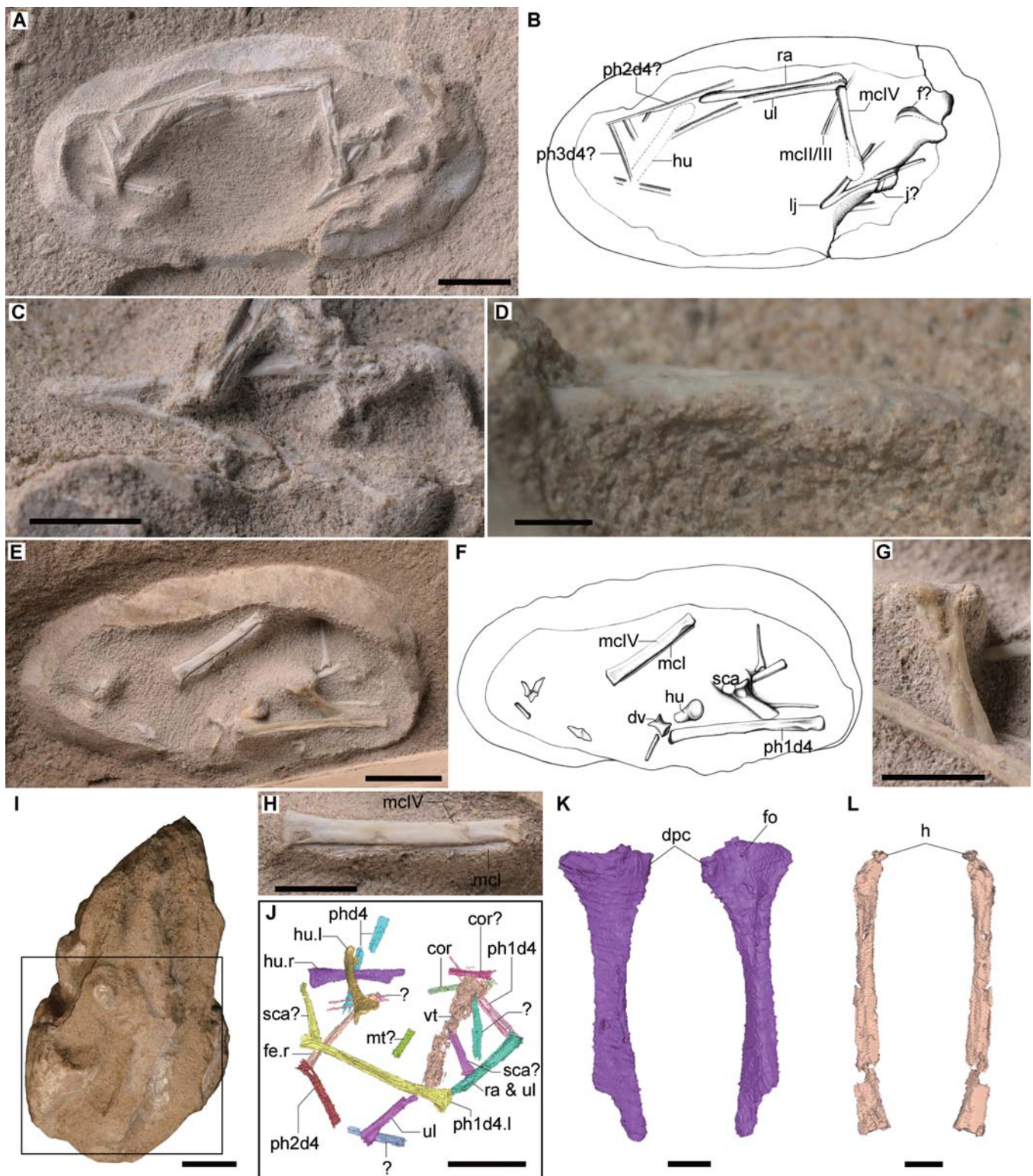


Fig. 3. Eggs with embryo. Embryo 12 (A to D), embryo 11 (E to H), embryo 13 (I to L). (A) and (B), photo and line drawing showing all elements of embryo 12 with the lower jaw exposed in ventral view; scale bar, 10 mm. (C) Close-up of the lower jaw; scale bar, 5 mm. (D) Close-up of the anterior portion of the lower jaw in left view; scale bar, 1 mm. (E) and (F), photo and line drawing showing all elements of embryo 11; scale bar, 10 mm. (G) Close-up of scapula; scale bar, 5 mm. (H) Close-up of metacarpal IV; scale bar, 5 mm. (I) Photo of embryo 13; scale bar, 10 mm.

(J) Interpretations of elements in the frame of (I), showing the position of embryo; scale bar, 10 mm. (K) Close-up of right humerus; scale bar, 2 mm. (L) Close-up of left femur; scale bar, 2 mm. Abbreviations: cor, coracoid; dpc, deltopectoral crest; dv, dorsal vertebra; f, frontal; fe, femur; fo, foramen; h, head; hu, humerus; j, jugal; l, left; lj, lower jaw; mcl-IV, metacarpal I-IV; mt, metatarsal; phd4, indeterminate wing phalanx; ph1-4d4, first to fourth phalanges of manual digit IV; r, right; ra, radius; sca, scapula; ul, ulna; vt, vertebra; ?, uncertain.

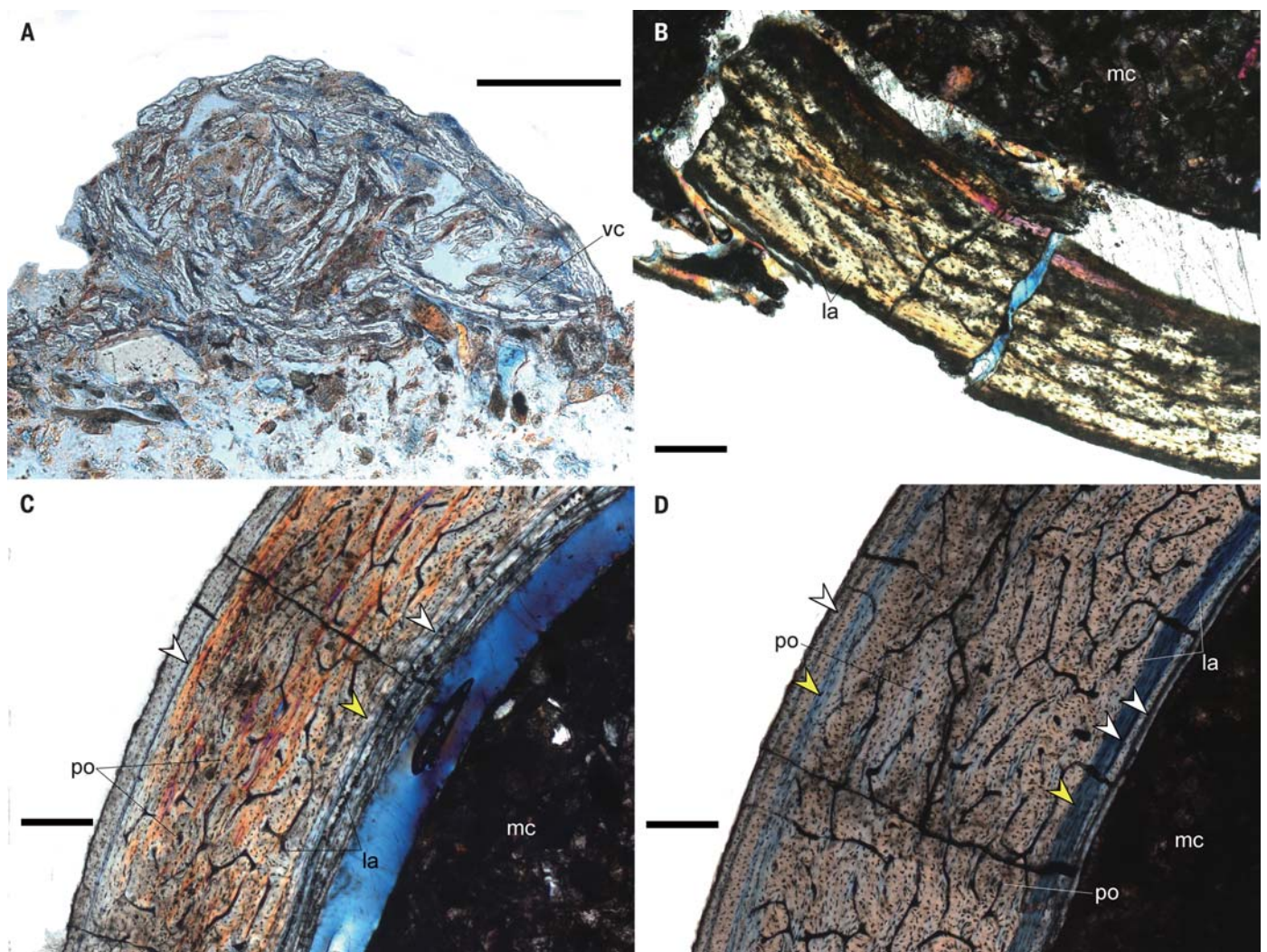


Fig. 4. Transverse mid-diaphyseal sections of ulnae under plane-polarized light. (A) Ulna of embryo 2, shown in fig. S2A; (B) ulna of IVPP V 18947.7 (estimated length ~130 mm); (C) ulna of IVPP V 18947.13 (estimated length ~140 mm); (D) ulna of IVPP V 18947.12

(estimated length ~190 mm). Scale bars, 200 μ m. White arrows indicate LAGs; yellow arrows indicate annuli. Abbreviations: la, lacuna; mc, medullary cavity; po, primary osteon; vc, vascular canal.

the same reptile species (10). Additionally, it is possible that some of these eggs were subjected to differential water uptake during transport.

Internal content could be observed in 42 eggs, either through computed tomography (CT) scanning or micropreparation. From these, 16 had embryonic remains (38% of the sample). Bones show a white color, are distributed along the egg (Fig. 3), and are not concentrated on the bottom half as observed in some dinosaurs (11, 12). With a few exceptions (movies S1 to S3), bones tend to be disarticulated and displaced from their natural position. The diameter of long bones, including wing phalanges, varies from 0.59 to 1.40 mm, most being slightly thinner than 1 mm. Where measurable, the bone cortex in long bones is around 0.15 to 0.20 mm, and thinner in cranial elements. No embryo is complete, with osteological material varying from one to several bones (Fig. 3 and figs. S1 to S7). This can be explained by

several factors, including the presence of embryos in distinct embryological stages, differential preservation of bones, and loss of elements during transport and burial, with part of the egg content expelled.

Establishing the developmental stages of the embryos is complex, with the length of comparable elements varying (tables S2 to S5). Three embryos (11, 12, and 13) have bones of similar sizes and likely represent the same developmental stage. In embryo 7, the humerus is about 20% longer than in embryo 13. The smallest isolated humerus found outside an egg, regarded to belong to a hatchling, is about 18 and 40% longer than that of embryos 7 and 13, respectively. The length of the deltopectoral crest along the shaft of the humerus varies between 25.5% to 27.8% in embryos and the hatchling, compared with 31.5 to 37.1% in subadults (table S5). The only other pterosaur where similar comparisons are possi-

ble is the archaeoptero-dactyloid *Pterodaustro*, in which the humerus of the hatchling is up to 20% longer than that of the embryo (5, 13) and the deltopectoral crest changes from around 23% in the embryo and hatchling to more than 30% in subadults, a pattern similar to the one recovered here. This suggests that the most complete embryos of *Hamipterus* (11 to 13) might be in an advanced developmental stage, but perhaps less than the sole of *Pterodaustro*.

Embryo 12 is the most complete one, containing a partial wing and cranial bones, including a complete lower jaw (~16.89 mm long). Dentaries are strongly connected (but unfused) for about 3.97 mm, occupying about 23% of the mandibular length. CT scanning did not reveal more cranial elements; not even the exposed elements could be distinguished from the matrix, suggesting that cranial bones were only starting to ossify, contrary to other parts of the skeleton

such as long bones and the vertebral column (movies S1 to S3).

Although the current available material cannot provide a complete view of the ontogenetic development of *Hamipterus*, and despite some uncertainty in regarding these embryos as representing late embryonic stages, some general observations can be made that considerably expand our knowledge about the embryology and ontogeny of pterosaurs (14). The skull roof was not well ossified before the animal hatched, albeit more than in birds (15) but less than in lepidosaurs (16) and crocodiles (17). Prior to hatching, the lower jaw already shows an anterior expansion that gets more developed during ontogeny. The symphyseal region increased from around 23% in embryos to 43 to 45% of the total lower jaw length in juveniles and subadults. No teeth were found in any of the embryos. Because teeth tend to be very resistant and embryos of dinosaurs (11), birds (18), and one pterosaur (3) show them, there seems to be no taphonomic explanation for their absence. Therefore, this embryo might be at a stage of development in ovo prior to teeth eruption, or dental eruption is delayed in this pterosaur, contrary to the condition found in lizards and crocodiles (19), the latter favored here.

Overall, wing elements show ossified shafts but still unformed articulations, such as the humerus and the wing metacarpal (Fig. 3, H and K). In two embryos, other metacarpals are also ossified despite being very thin, with metacarpal I reaching the carpus. No extensor tendon process was identified, suggesting that it ossifies only slightly before or after hatching. The deltopectoral crest is warped in juveniles but not in the embryos, indicating that its distal end was still cartilaginous. This suggests that the most powerful wing depressor, *m. pectoralis* (20), which is attached to the deltopectoral crest, was not well developed in neonates. The embryonic scapula lacks a *processus scapularis* (Fig. 3G), which is the origin of *m. teres major*, a muscle involved in the elevation of the wing (20). This structure is observed in the smallest nonembryonic individual recovered, in which the scapula is slightly more than four times as longer than in the embryos. The femur, on the contrary, is well developed, showing the typical pterosaurian femoral head, with a constricted neck and complete distal articulation (Fig. 3I). This suggests that the hind limbs have developed more rapidly compared to the forelimbs and might have been functional right after the animal hatched. Thus, newborns were likely to move around but were not able to fly, leading to the hypothesis that *Hamipterus* might have been less precocious than advocated for flying reptiles in general (6) and probably needed some parental care.

Osteohistological sections of some postcranial elements from embryos and larger-sized individuals were made (Fig. 4 and figs. S8 to S10). None showed plywood-like bone, which is regarded as unique for pterosaurs (21). Secondary osteons, which are rare in these flying reptiles

(22), are also lacking. In the embryo, the cortex of all three sectioned bones (radius, ulna, and one wing phalanx) is composed of woven bone, with large vascular canals, which indicates fast growth (23). Regarding nonembryonic elements found scattered in the matrix, osteohistological sections of three ulnae were made. The smallest shows fibrolamellar bone without any growth mark, suggesting that it belonged to a young individual. The second (~140 mm) also shows fibrolamellar bone, but presents internal circumferential layers (ICLs) with one line of arrested growth (LAG) and an annulus, suggesting that growth of the medullary cavity had ceased (23). Another LAG can be found in the outermost part of the periosteal bone matrix, but no external fundamental system (EFS) (1) was developed. This configuration has been interpreted as an indicator of sexual maturity (24). In the largest ulna (~190 mm), the ICLs are also present, and one LAG and an annulus are placed in the outermost part of cortex, but no EFS is formed yet. Based on the presence of growth marks (LAG and annulus) and the absence of any sign of bone remodeling or secondary structures (23) that could erase those marks, this bone might represent an individual at least 2 years old, still growing at the time of its death.

The main locality where eggs have been collected is characterized by a succession of white to gray, middle- to fine-grained sandstones that were deposited in a fluvio-lacustrine environment (fig. S12). Localized lenses of mudstone are present (fig. S13). Egg- and bone-carrying layers have a thickness between 10 to 30 cm and show extensive mudstone pellets. In a 2.2-m section, eight layers with pterosaur bones have been identified, four of which show egg concentrations in a vertical distance of 1.4 m. This sedimentological data, associated with the exceptional quantity of eggs and bones, indicate that events of high energy such as storms have passed over a nesting site, causing the eggs to be moved inside the lake where they floated for a short period of time, becoming concentrated and eventually buried along with disarticulated skeletons. Our findings further demonstrate the exceptional conditions necessary for the preservation of such fragile material and can explain the notable paucity of pterosaur eggs and embryos in the paleontological record compared to other reptiles (25), because the preservation potential of soft-shelled specimens is regarded as very poor (26). Furthermore, this occurrence implies colonial breeding for *Hamipterus tianshanensis*, as demonstrated by the osteohistological identification of individuals in different growth stages, a hypothesis speculated for pterosaurs before on the basis of very limited evidence (7). The large quantities of specimens, and now eggs, indicate that gregarious behavior might have been widespread among derived pterosaurs.

REFERENCES AND NOTES

1. A. W. A. Kellner et al., *An. Acad. Bras. Cienc.* **85**, 113–135 (2013).

2. X. Wang et al., *An. Acad. Bras. Cienc.* **87**, 1599–1609 (2015).
3. X. Wang, Z. Zhou, *Nature* **429**, 621 (2004).
4. Q. Ji et al., *Nature* **432**, 572 (2004).
5. L. M. Chiappe, L. Codorniu, G. Grellet-Tinner, D. Rivaola, *Nature* **432**, 571–572 (2004).
6. D. M. Unwin, D. C. Deeming, *Zitteliana* **28**, 199–207 (2008).
7. G. Grellet-Tinner et al., *Geoscience Frontiers* **5**, 759–765 (2014).
8. X. Wang et al., *Curr. Biol.* **24**, 1323–1330 (2014).
9. D. M. Martill, *Curr. Biol.* **24**, R615–R617 (2014).
10. H. Schleich, W. Kästle, *Reptile Egg-Shell SEM Atlas* (Gustav Fisher Verlag, Stuttgart, 1988).
11. L. M. Chiappe et al., *Nature* **396**, 258–261 (1998).
12. R. R. Reisz, D. Scott, H. D. Sues, D. C. Evans, M. A. Raath, *Science* **309**, 761–764 (2005).
13. L. Codorniu, L. M. Chiappe, *Can. J. Earth Sci.* **41**, 9–18 (2004).
14. A. W. A. Kellner, *An. Acad. Bras. Cienc.* **87**, 669–689 (2015).
15. M. J. Stark, *Structural Variants and Invariants in Avian Embryonic and Postnatal Development*. In Starck, J.M. & Ricklefs, R.E. (Eds.), *Avian Growth and Development. Evolution within the altricial precocial spectrum* (Oxford Univ. Press, New York, 1998).
16. O. Rieppel, *J. Herpetol.* **28**, 145–153 (1994).
17. O. Rieppel, *J. Zool. (Lond.)* **109**, 301–325 (1993).
18. Z. Zhou, F. Zhang, *Science* **306**, 653 (2004).
19. B. Westergaard, M. W. J. Ferguson, *J. Zool. (Lond.)* **212**, 191–222 (1987).
20. S. C. Bennett, *Geol. Soc. Lond. Spec. Publ.* **217**, 191–215 (2003).
21. J. R. Horner, K. Padian, A. D. Ricqlés, *Paleobiology* **27**, 39–58 (2001).
22. J. M. Sayão, *Geol. Soc. Spec. Publ.* **217**, 335–342 (2003).
23. L. Steel, in *Flugsaurier: Pterosaur papers in honour of Peter Wellnhofer, E. Buffetaut, D. W. E. Hone, Eds.*, Special volume: *Zitteliana, B*, **28**, 109–125 (2008).
24. A. Chinsamy, L. Codorniu, L. Chiappe, *Biol. Lett.* **4**, 282–285 (2008).
25. K. Carpenter, K. F. Hirsh, J. R. Horner, *Dinosaur Eggs and Babies* (Cambridge Univ. Press, Cambridge, 1994).
26. K. F. Hirsh, *Vertebr. Paleontol.* **16**, 752–762 (1996).

ACKNOWLEDGMENTS

We thank L. Xiang, H.-J. Zhou, and R.-J. Wang [Institute of Vertebrate Paleontology and Paleoanthropology, Chinese Academy of Sciences (CAS)] for the preparation of the specimens, W. Gao for photography, A.-J. Shi for line drawings, and Y.-M. Hou and P.-F. Yin for help with the CT scan and reconstruction (IVPP). We are also indebted to Y. Li, L. Xiang, Q.-G. Liu, R.-J. Wang, H.-J. Zhou, W. Gao, H.-Q. Shou (IVPP), and G.-L. Wu, B.-L. Guan, H.-M. Wu, Q.-J. Li, H.-Y. Chen, F. Yan, Y.-L. Tian, Z.-J. Yin, H.-P. Dai, and J. Tong (Hami) for assistance in the field work. This study was supported by the National Natural Science Foundation of China (41572020, 41688103, 41602011, 91514302, and 40825005), the Strategic Priority Research Program (B) of CAS (XDB18000000), the Hundred Talents Project of CAS, the Excavation Funding and Emphatic Deployed Project of IVPP, CAS. T.R. acknowledges funding from the Fundação de Amparo à Pesquisa e Inovação do Espírito Santo (FAPES no. 67678254) and the Conselho Nacional de Desenvolvimento Científico e Tecnológico (CNPq no. 460784/2014-5); and A.W.A.K. from the Fundação Carlos Chagas Filho de Amparo à Pesquisa do Rio de Janeiro (FAPERJ no. E-26/202.893/2015) and the Conselho Nacional de Desenvolvimento Científico e Tecnológico (CNPq no. 304780/2013-8). All specimens are housed at the Institute of Vertebrate Paleontology and Paleoanthropology in Beijing, China.

SUPPLEMENTARY MATERIALS

www.sciencemag.org/content/358/6367/1197/suppl/DC1
Figs. S1 to S13
Tables S1 to S5
Movies S1 to S3
References (27, 28)

14 March 2017; resubmitted 15 July 2017
Accepted 26 October 2017
10.1126/science.aan2329